





Article

Influence of the Type and the Amount of Surfactant in Phillipsite on Adsorption of Diclofenac Sodium

Danijela Smiljanić ¹, Aleksandra Daković ^{1,*}, Milena Obradović ¹, Milica Ožegović ¹, Marija Marković ¹, George E. Rottinghaus ² and Bruno de Gennaro ³

¹ Institute for Technology of Nuclear and Other Mineral Raw Materials, Franche D' Epere 86, 11000 Belgrade, Serbia

² Veterinary Medical Diagnostic Laboratory, College of Veterinary Medicine, University of Missouri, Columbia, MO 65211, USA

³ ACLabs—Applied Chemistry Labs, Department of Chemical, Materials Engineering and Industrial Production, University of Naples Federico II, P.le V. Tecchio 80, 80125 Naples, Italy

* Correspondence: a.dakovic@itnms.ac.rs

Abstract: Modified phillipsite samples were prepared with two different amounts (monolayer and bilayer coverage) of surfactants octadecyldimethylbenzylammonium chloride (O) and dodecylamine (D). Composites were characterized by Fourier transform infrared spectroscopy with attenuated total reflectance (FTIR–ATR), thermal analysis and determination of zeta potential, and subsequently tested for removal of diclofenac sodium (DCF). Drug adsorption experiments were performed under different initial DCF concentrations and different contact times. In order to investigate the influence of the chemical structure of surfactants used for modification of phillipsite on the preparation and properties of composites and DCF adsorption, experimental data were compared with previously published results on DCF adsorption by composites containing phillipsite and the same amounts of surfactants cetylpyridinium chloride (C) and Arquad[®]2HT-75 (A). DCF adsorption isotherms for O and D composites showed a better fit with the Langmuir model with maximum adsorption capacities between 12.3 and 38.4 mg/g and are similar to those for C and A composites, while kinetics run followed a pseudo-second-order model. Composites containing either benzyl or pyridine functional groups showed higher adsorption of DCF, implying that surfactant structure has a significant impact on drug adsorption. Drug adsorption onto O, D, C and A composites was also confirmed by FTIR–ATR spectroscopy and zeta potential measurements.

Keywords: zeolite-rich tuff; phillipsite; surfactant modification; drug adsorption; diclofenac



Citation: Smiljanić, D.; Daković, A.; Obradović, M.; Ožegović, M.; Marković, M.; Rottinghaus, G.E.; de Gennaro, B. Influence of the Type and the Amount of Surfactant in Phillipsite on Adsorption of Diclofenac Sodium. *Catalysts* **2023**, *13*, 71. <https://doi.org/10.3390/catal13010071>

Academic Editor: Aurora Santos

Received: 30 November 2022

Revised: 23 December 2022

Accepted: 26 December 2022

Published: 30 December 2022



Copyright: © 2022 by the authors. Licensee MDPI, Basel, Switzerland. This article is an open access article distributed under the terms and conditions of the Creative Commons Attribution (CC BY) license (<https://creativecommons.org/licenses/by/4.0/>).

1. Introduction

Zeolites are aluminosilicate minerals with a three-dimensional framework consisting of SiO₄ and AlO₄ tetrahedra linked through shared oxygen atoms in a regular way creating cavities and channels. Due to the isomorphic substitution of Si⁴⁺ with Al³⁺, the zeolitic structure has a net negative charge that is compensated by exchangeable cations located in channels and at the zeolitic surface together with water molecules [1,2]. Besides being abundant and eco-friendly, natural zeolites are also reasonably priced and have a high cation exchange capacity, physicochemical stability, and good hydraulic properties [3–5]. Due to the cation exchange property, these minerals have received substantial attention for the removal of heavy metal cations and ammonium from various systems, making them a potential solution in environmental cleaning processes [5–11]. However, because of the net negative charge and the presence of inorganic cations in the zeolite structure, these minerals are hydrophilic and have no affinity for the adsorption of anions and/or hydrophobic molecules [12,13]. By using large organic cations, such as surfactant, to modify the zeolitic surface, this restriction can be overcome. Surfactant molecules are too large to enter into zeolite channels or access internal cation exchange sites, so their adsorption is limited only

to the external zeolitic surface. The amount of inorganic cations at the external surface that can be replaced with long-chain organic cations is expressed as the external cation exchange capacity (ECEC) of zeolite. Depending on the amount of surfactant used for modification of the zeolitic surface, their adsorption onto a negatively-charged surface involves both cation exchange and hydrophobic bonding. The surface charge of the composite will vary depending on how much surfactant is employed for the functionalization. If the amount of surfactant corresponds to 100% of the zeolite's ECEC value, a monolayer is created, providing hydrophobic sites at zeolite surface, thus surface charge changes from negative to neutral. If the amount of surfactant is above 100% of the ECEC of zeolite, tail-to-tail interaction of surfactant molecules will lead to formation of surfactant bilayer. In the bilayer case, cationic surfactant heads in the outer surfactant layer make zeolitic surface positive and will provide adsorption sites for anionic species [13–15].

Surfactant-modified zeolites have been widely researched for the removal of various pollutants from the aquatic environment, for example, anionic species of metals (such as chromates and arsenates), organic compounds (benzene, ethylbenzene, toluene, xylene, chlorophenol, perchloroethylene, dyes, pesticides, bisphenol A, etc.), pathogens [5,7,12,16–27] and more recently nonsteroidal anti-inflammatory drugs (NSAIDs) [13,28,29]. Diclofenac (DCF) is an over-the-counter drug from the class of NSAIDs frequently used, in both human and animal medicine, to treat various pain states and fevers [30,31]. As a result, increased consumption causes environmental contamination due to release in water systems [32–36]. Diclofenac caught worldwide attention as a contaminant in 2004 when a large number of vulture deaths were reported in the Indian subcontinent. Vultures died from kidney failure after being fed with carcasses of cows that were treated with diclofenac before death. In 2006, countries on the Indian subcontinent began banning diclofenac in veterinary medicine, and after this measure, the vulture population increased substantially [33,37,38]. In 2013, in Europe, DCF was added to the first Watch List of contaminants of emerging concern (Directive 2013/39/EU (Article 8b)) in order to gather the data needed to assess this drug's potential for pollution of the environment [35]. Recently, in the review of Bonnefille et al. (2018), it was reported that prolonged exposure of different marine organisms to DCF (even at concentrations in ng/L) causes a variety of effects, including the modification of vital biological functions [39]. This suggests that chronic exposure should not be lightly disregarded. Thus, it is necessary to find an economical way to remove DCF from wastewater before discharge into the environment. The literature data reported a high potential of minerals treated with surfactants for DCF adsorption and that increase in surfactant concentration at the mineral's surface (zeolites) or in minerals (clays) resulted in greater drug adsorption [13,29,40–43].

In a previous paper [29], results on the adsorption of DCF and ketoprofen onto composites prepared by modification of two zeolites (clinoptilolite and phillipsite) with two different amounts (monolayer and bilayer coverage) of surfactants—cetylpyridinium chloride (C) and Arquad[®]2HT-75 (A) were presented. Results showed that adsorption of both drugs increased with increasing the amount of each surfactant at zeolite surfaces and with increasing the initial concentration of each drug. It was determined that depending on the zeolitic content in the zeolitic tuff, the type and the number of surfactants and the type of the drug, the characteristic adsorption capacity of investigated composites varied from 1 to 35 mg/g. Moreover, composites of clinoptilolite and phillipsite with C gave higher adsorption of DCF and ketoprofen.

The present study aims to examine if composites of phillipsite-rich tuff with octadecyl-dimethylbenzylammonium chloride (O) and dodecylamine (D) (in amounts of 100% and 200% of ECEC values) are able to adsorb the nonsteroidal anti-inflammatory drug DCF. The prepared composites were used for the first time for DCF adsorption, and the adsorption of the drug onto composites containing aliphatic primary amine—D and quaternary ammonium salt with aromatic ring—O was compared. Additionally, since generally, surfactant ions in composites are responsible for the adsorption of drugs and their adsorption is dependent on the type of surfactant used for modification of the zeolitic surface, results were

discussed together with previous results on adsorption of DCF on composites of phillipsite with C (quaternary ammonium salt with pyridine ring) and A (quaternary ammonium salt with two alkyl chains) [29]. The main aim of this research is to investigate the influence of the chemical structure of surfactants used for modification of the phillipsite surface on the preparation and properties of composites and subsequent DCF adsorption.

The DCF adsorption experiments on O and D composites were performed in batch conditions, testing the influence of different initial drug concentrations and contact time. The mechanism of DCF adsorption by composites was suggested based on the drug adsorption experiments. Detailed characterization of surfactant-modified zeolites was performed by several characterization methods: FTIR-ATR analysis, thermal analysis, and zeta potential measurements. Additionally, to confirm the presence of the DCF at the modified zeolitic surfaces, composites containing the adsorbed drug were characterized by using FTIR-ATR spectroscopy and zeta potential measurements.

2. Results and Discussion

2.1. Characterization of O and D Composites

FTIR-ATR spectra of starting material—P, surfactants—O and D, and composites PO100, PO200, PD100 and PD200 are given in Figure 1A,B. Infrared analysis of P has displayed typical adsorption bands of zeolite-rich tuff associated with internal and external framework vibration of primary and secondary building units [15,29,44,45].

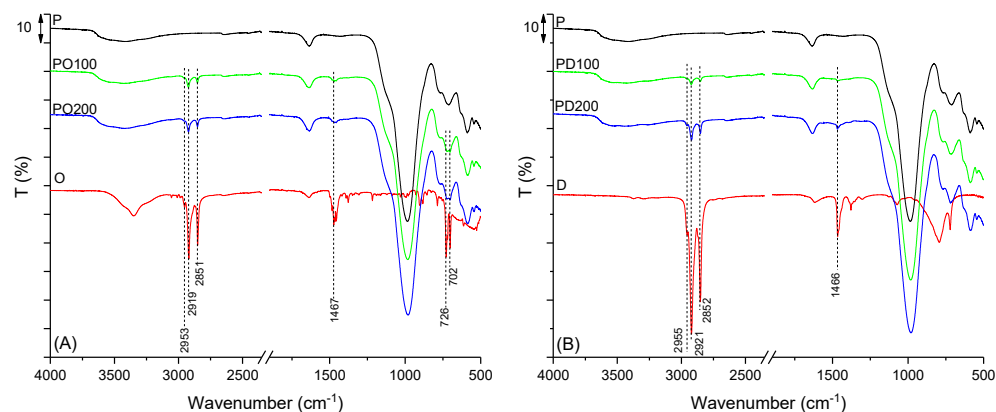


Figure 1. FTIR-ATR spectra of (A) starting material—P, surfactant octadecyldimethylbenzylammonium chloride—O, and composites PO100 and PO200; (B) starting material—P, surfactant dodecyl amine—D, and composites PD100 and PD200.

A broad peak at around 3500 cm^{-1} and a smaller one at 1635 cm^{-1} belong to O-H stretching and bending vibrations in water molecules, respectively. A high-intensity peak at 985 cm^{-1} originates from asymmetric stretching vibrations of the T-O group, where T stands for Al or Si and O is an oxygen atom. Additionally, T-O-T stretching and bending vibrations are confirmed with peaks below 800 cm^{-1} [44]. All bands characteristic for P are also evident in the spectra of composites, proving that the functionalization process and presence of surfactant molecules in composites did not cause any changes in the structure of the tuff. After modification with O, in the spectra of composites (PO100 and PO200), new peaks have appeared (Figure 1A), proving the presence of surfactant molecules. The peak at 2953 cm^{-1} belongs to the CH_3 group, whereas peaks at 2919 cm^{-1} and 2851 cm^{-1} are due to asymmetric and symmetric C-H stretching vibrations of CH_2 groups in the surfactant alkyl chain, respectively. Additionally, the low-intensity peak at 1467 cm^{-1} is from C-H bending vibrations. Peaks at 726 and 702 cm^{-1} are associated with vibrations of C-H groups in the benzene ring of O molecules [46]. When D was used for phillipsite's surface modification (Figure 1B), peaks associated with surfactant were visible at 2955 cm^{-1} , 2921 cm^{-1} , and 2852 cm^{-1} (C-H stretching vibration), as well as at 1466 cm^{-1} (bending C-H vibration). It is observed that intensities of peaks indicative of the surfactant presence

increased with increasing the surfactant content at the zeolitic surface, thus confirming that FTIR spectroscopy served to validate successful modification of the zeolite's surface with no changes of the zeolitic structure. Similar peaks were reported for composites of phillipsite with C and A (PCM, PCB, PAM, and PAB) when bands originating from C-H stretching and bending vibrations confirmed successful modification of phillipsite-rich tuff with C or A in amounts of 100 and 200% of ECEC [29].

Thermal analysis (DSC/TGA) was used to study the thermal properties of the starting material and prepared composites, as well as to supply information on the bonding between organic species and P. The differential scanning calorimetry (DSC) curves of P and composites (PO100, PO200, PD100, and PD200) are presented in Figure 2, while the mass loss from thermogravimetric (TGA) curves for all samples in different temperature regions is given in Table 1.

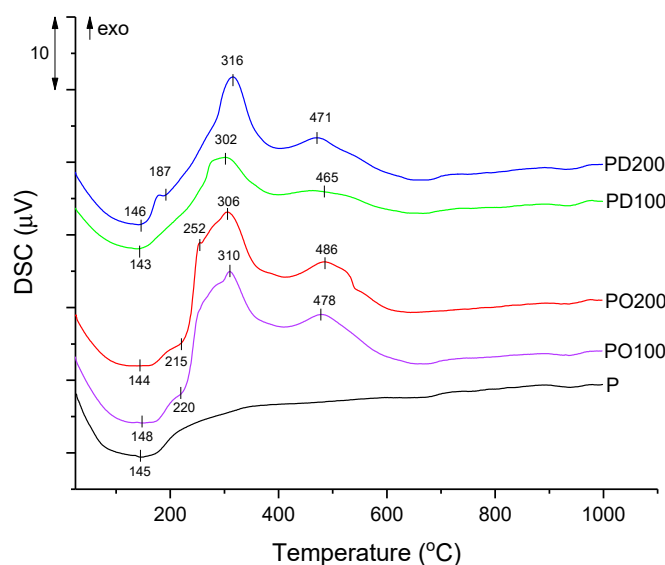


Figure 2. DSC analysis of starting material—P and composites PO100, PO200, PD100 and PD200.

Table 1. Mass loss (%) from TGA curves for starting material-P and composites.

Sample	Mass Loss (%)			
	25–200 °C	200–700 °C	700–1000 °C	∑25–1000 °C
P	7.44	3.77	0.08	11.29
PO100	6.46	8.02	0.07	14.55
PO200	6.35	11.35	0.03	17.73
PD100	6.47	5.94	0.04	12.45
PD200	7.49	6.98	0.05	14.52

Based on the results given in Table 1 and TGA curves (not shown), for P, a continuous mass loss in the temperature range of 25–1000 °C is observed, and the total mass loss was 11.29%. The presence of both surfactants led to an increase in the mass loss and was proportional to the amount of surfactant molecules at P surface, meaning that mass loss for composites increased with increasing the amount of each surfactant at the P surface. Thus, in the case of PO100 and PO200, total mass losses were 14.55% and 17.73%, respectively, while in the case of D composites PD100 and PD200, mass losses were 12.45% for PD100 and 14.52% for PD200. These results were in agreement with the literature and confirmed the presence of surfactants at the P surface.

From Table 1, it can also be seen that for P, most of the mass loss occurred up to 200 °C (7.44%) and is associated with physically adsorbed water. Usually, in this region, for composites of zeolite containing surfactants in amounts up to 100% of ECEC, due to the increased hydrophobicity of the zeolitic surface, the mass loss should be lower. When

the amount of surfactant at the zeolitic surface is above 100% ECEC, besides dehydration from physically adsorbed water, mass loss is also associated with the desorption of non-adsorbed organic compound or elimination of weakly bound surfactant. After modification with surfactants, mass loss in the first temperature region for PO100, PO200 and PD100 was slightly lower (around 6.40%) compared to the mass loss for P (7.44%), confirming hydrophobicity of composites surfaces. Composite PD200 showed a mass loss (7.49%) similar to the mass loss of P, suggesting the desorption of a small fraction of unbound D molecules [47,48]. In the second temperature range from 200–700 °C, P continued to gradually lose water molecules coordinated to the cations in zeolite channels (mass loss of 3.77%), while for composites, mass loss mainly originates from the oxidation of organic phase present at the zeolitic surface. It is observed that for composites, mass loss increased with increasing the amount of O and D in composites. Thus, PO100 had a mass loss of 8.02%, and PO200 had a mass loss of 11.35%, while for D composites, PD100 and PD200, mass loss was 5.94% and 6.98%, respectively. Additionally, higher mass losses were reported in the case of composites with O (PO100 and PO200) due to the higher molecular weight of the O molecule.

The DSC curve of P showed only one visible wide endothermic peak (with a maximum of around 145 °C) originating from the desorption of water molecules. Besides the peak around 145 °C, composites PO100, PO200 and PD200 have additional low-intensity shoulder, around 220 °C, 215 °C, and 187 °C respectively, that may be connected to the loss of non-adsorbed or loosely bound surfactant molecules. In the case of PD200, this shoulder appeared below 200 °C (187 °C), suggesting that this composite desorption of weakly bound D occurred at a lower temperature and is confirmed by the slightly higher mass loss in the first temperature region. DSC analysis has shown that in composites, between 200–700 °C, exothermic peaks occurred due to the oxidation of the organic phase present at the P surface. When O was used for modification in the amount equal to 100% of ECEC (PO100), exothermic peaks at 310 °C and 478 °C were observed, while with an increase of the amount of surfactant (PO200), a small peak at 252 °C and more intensive exothermic peaks at 306 °C and 486 °C were noticed, suggesting the higher energy requirements to burn higher surfactant amount [48]. Similar behavior was noticed for composites with D: DSC curves showed exothermic peaks at 302 °C and 465 °C for PD100, while for PD200, these peaks were at 316 °C and 471 °C. Again, the more intensive peak was in the case of composite with a higher surfactant amount (PD200). DSC curves of O and D composites showed that intensities of the exothermic peaks for PD100 and PD200 were noticeably lower than for PO100 and PO200, being a consequence of the higher molecular weight of the O molecule.

Zeta potential is a reflection of surface potential, and it changes depending on surfactant loading at the zeolite surface [13]. When surfactants are used in an amount equal to 100% of ECEC, zeta potential should be close to zero indicating increased surface hydrophobicity, while when the amount of surfactants is equal to 200% of ECEC, a bi-layer of surfactant should be formed at the zeolite surface making the composite surface more positive. This means that surfactant molecules are covering negative active sites at the zeolite surface and, in this way, are reducing the negative zeta potential value of unmodified zeolite.

Zeta potential data for P and O and D composites (see Section 2.3) showed that the initial negative surface of P (−34.0 mV) after modification with O turned to positive (+2.3 mV for PO100 and +20.2 mV for PO200) while after modification with D, the negative charge of P was changed to less negative as the amount of D increased in D composites (−14.1 mV for PD100 and to −12.6 mV for PD200). For both types of composites, zeta potential values confirmed successful modification and the presence of O and D at the surface of P. It is also observed that changes in zeta potential value are more pronounced in the case of quaternary ammonium ion—O, than in the case of modification with primary amine—D.

In the case of O composites, when the amount of O was equal to ECEC value (PO100), zeta potential approached zero, confirming nearly monolayer formation and almost complete hydrophobicity of the P surface. At O amount equal to 200%, ECEC zeta potential became positive, pointing charge reversal and bilayer formation at the P surface. Similar changes in zeta potential values were noticed when P was modified with the same amounts of quaternary ammonium surfactants C and A. When the amount of these surfactants was equal to 100% ECEC, zeta potential became slightly positive (+2.8 mV for PCM, and +2.1 mV for PAM), while when the amount of C and A was 200% of ECEC reversed charge was reported (+30.6 mV for PCB, and +33.5 mV for PAB) [29]. These results indicated that although these quaternary ammonium salts have different functional groups and different chain lengths: O (one alkyl chain with C₁₈), C (one alkyl chain with C₁₆) and A (two alkyl chains with C_{14–18}), they have the same effect on zeta potential meaning that they are similarly positioned at the P surfaces. However, when primary amine—D was used, zeta potential after modification remained negative for composites PD100 and PD200, and these results may be explained by its different chemical structure, much shorter chain length (one alkyl chain with C₁₂) and smaller cationic head. The negative values of zeta potential mean that despite primary amine being adsorbed at P surfaces, due to the much smaller chain length, the P surface is still partially uncovered. Results of zeta potential measurements for O and D composites suggest that although equivalent amounts of the organic phase (O and D) were used for modification, differences in surfactant molecular structures will lead to different arrangements of the surfactant molecules at composite surfaces [49]. Similar differences in zeta potential values were reported by Orta et al. (2019) [50] when montmorillonite (Mt) was modified with quaternary ammonium ion octadecyltrimethylammonium (ODTMA) and primary amine octadecylamine (ODA) in two different amounts 50 and 100% of ECEC. Namely, the authors noticed that zeta potential changes from negative (for Mt) to positive for modification with ODTMA, while when ODA was used for modification, the surface of Mt remained negative. The behavior of composite with primary amine was explained with the smaller size of the ammonium head groups in the ODA ($-\text{NH}_3^+$) compared to the size of ODTMA ($-\text{N}(\text{CH}_3)_3^+$). They also indicated that primary ammonium head groups might form additional hydrogen bonds with water molecules and chloride anions onto the clay surface, and consequently, if a positive surface charge is generated, it would be almost neutralized [50].

2.2. Adsorption of Diclofenac Sodium

Adsorption isotherms are a crucial step in figuring out the tested materials' adsorptive capacities and determining the DCF adsorption mechanism. In Figure 3, adsorption isotherms of DCF from buffer solution on O and D composites are presented. For all composites, adsorption of DCF increased with increasing the initial drug concentration and with increasing the amount of organic phase in both types of composites. This means that either quaternary ammonium ion or primary amine at the surface of P is responsible for the adsorption of DCF by O and D composites since unmodified P has no affinity for the adsorption of this drug. It is noticed that drug adsorption increased in the following order: PO200 > PD200 > PO100 > PD100, making it simpler to see that bilayer composites had a higher adsorption capacity than monolayer composites. Also, comparing the adsorption of DCF by O and D composites containing the same amount of organic phase, composites containing quaternary ammonium ion are more efficient for the adsorption of DCF than composites with primary amine. Under the applied experimental conditions, the maximum adsorbed amounts of DCF by O and D composites with an amount of O or D equal to 100% ECEC were 11.1 mg/g for PD100 and 19.9 mg/g for PO100. For composites with an organic phase equal to 200% of ECEC, the adsorption of DCF was 26.8 mg/g and 37.9 mg/g for PD200 and PO200, respectively.

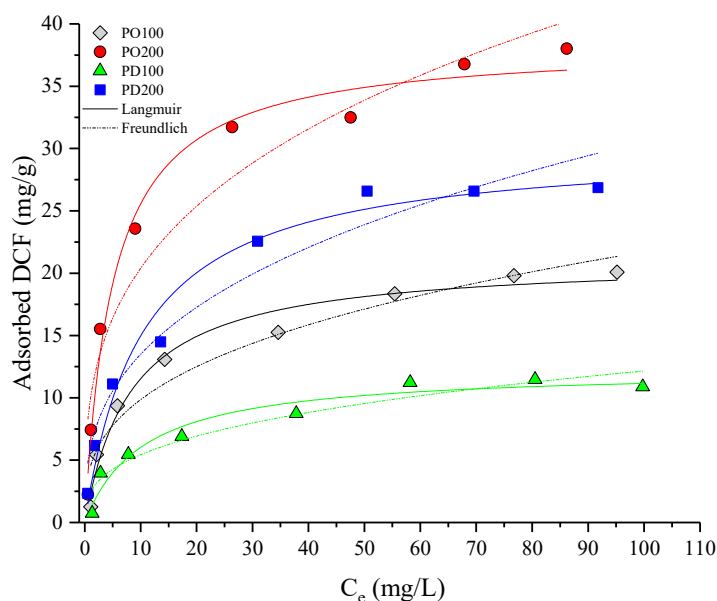


Figure 3. Equilibrium isotherms of DCF adsorption on composites of P.

Since the adsorption of DCF followed nonlinear isotherms, Langmuir and Freundlich isotherm models (Equations (1) and (2), respectively) were applied to fit the experimental data:

$$Q_e = \frac{Q_{max}K_L C_e}{1 + K_L C_e} \quad (1)$$

$$Q_e = K_F C_e^{1/n} \quad (2)$$

where Q_e (mg/g) is the amount of loaded DCF at equilibrium, C_e (mg/L) is the concentration of DCF in solution at equilibrium, Q_{max} (mg/g) is the highest concentration of the drug, K_L (L/mg) and K_F (L/mg) are Langmuir and Freundlich constants, respectively, and $1/n$ is a constant related to the strength of adsorption [51].

Due to the Langmuir isotherm's (Equation (1)) presumption that adsorbate molecules can only form one layer, the curve reaches a plateau [28,29]. Freundlich isotherm (Equation (2)) takes into consideration the heterogeneity of adsorbents represented by the constant n in the Freundlich equation [18]. According to the n constant, the favorability of adsorption can be estimated: values above 2 represent good, between 1–2 medium, and below 1 poor adsorbate-adsorbent interactions [18,52]. The determination coefficients (R^2) and Akaike weight parameter (AIC_w) were used to evaluate the selected mathematical models [53,54]. For all composites, obtained n values were higher than 2, suggesting good affinity of O and D composites for DCF adsorption. The computed adsorption isotherm parameters are listed in Table 2. Both mathematical models, Langmuir and Freundlich, had R^2 above 0.9, suggesting good agreement with experimental data. However, according to slightly higher R^2 and based on AIC_w values, the Langmuir model consistently provided a better fit.

The adsorption of DCF on several surfactant-modified zeolites was also found to exhibit nonlinear isotherms that are in good agreement with the Langmuir isotherm model [29,43,47,48]. The results of this study (Figure 3) and a review of the literature both point to nonlinear isotherms for the adsorption of DCF. It was previously mentioned that the adsorption of DCF may be dependent on the type of organic phase used for the modification of the P surface. In a previous study, the adsorption of DCF by composites containing the same amounts of C and A (100 and 200% ECEC) was studied under the same experimental conditions. Composites with C and A amounts equal to 100% of ECEC were denoted as PCM and PAM, while composites with surfactants amounting equal to 200% ECEC were denoted as PCB and PAB. It was observed that the adsorption of DCF increased with increasing the amount of each surfactant in composites as well as with increasing

the initial concentration of DCF. In all cases, nonlinear adsorption isotherms described the adsorption of DCF by C and A composites. From Langmuir isotherms (Table 3), maximum adsorption capacities for monolayer composites were 17.2 mg/g for PCM and 7.4 for PAM, while for bilayer composites, adsorption of the drug was 30.0 mg/g and 19.9 mg/g for PCB and PAB, respectively. Comparing the results of DCF adsorption by composites containing C and A with those for adsorption of the drug by O and D composites, for monolayer composites, adsorption of DCF increased, depending on the type of organic phase, in the following order $A < D < C < O$. The highest adsorption of DCF by monolayer composites were obtained with O (one alkyl chain with C_{18})—21.1 mg/g and C (one alkyl chain with C_{16})—17.2 mg/g, suggesting that longer chain but also the presence of aromatic rings (benzyl in O and pyridine in C) in their structure contribute to the higher adsorption of DCF that also has aromatic ring [41,43]. Lower adsorption of DCF by PD100 (12.3 mg/g) can be explained by the shorter alkyl chain in the D structure. However, although A has two alkyl chains with relatively high lengths (C_{14-18}), its monolayer resulted in the lowest DCF adsorption (7.4 mg/g). Composites containing C, O and D in the amount of 200% ECEC showed similar adsorption of DCF (30.0 mg/g for PCB, 38.8 mg/g for PO200 and 30.8 mg/g for PD200), while only composite PAB showed much lower adsorption of DCF (19.9 mg/g). It is possible that the presence of two alkyl chains in A hindered DCF adsorption by composites PAM and PAB.

Table 2. Mathematical models for the adsorption isotherms: parameters and goodness-of-fit.

Drug	Sample	Model	Parameters			Goodness-of-Fit	
			K (L/mg)	n	Q_{max} (mg/g)	R^2	AICw
DCF	PO100	Langmuir	0.12 ± 0.03		21.1 ± 0.9	0.974	0.974
		Freundlich	4.5 ± 0.8	2.9 ± 0.4		0.937	0.026
	PO200	Langmuir	0.20 ± 0.04		38.4 ± 0.9	0.984	0.998
		Freundlich	9.9 ± 0.9	3.7 ± 0.3		0.925	0.002
	PD100	Langmuir	0.10 ± 0.03		12.3 ± 0.8	0.947	0.852
		Freundlich	2.4 ± 0.5	2.9 ± 0.4		0.919	0.148
	PD200	Langmuir	0.14 ± 0.05		30.2 ± 0.7	0.974	0.918
		Freundlich	0.10 ± 0.03	2.8 ± 0.4		0.952	0.082

Table 3. DCF adsorption on P composites with different surfactants.

Surfactant Amount	Surfactant Type	* Adsorbed DCF mg/g	Reference
100% of ECEC	C	17.2	[29]
	A	7.4	[29]
	O	21.1	This study
	D	12.3	This study
200% of ECEC	C	30.0	[29]
	A	19.9	[29]
	O	38.8	This study
	D	30.8	This study

* Langmuir model values.

DCF is a hydrophobic molecule that exists in anionic form at pH levels above 3. Thus, nonlinear isotherms obtained for O, D, C and A composites suggest a complex adsorption mechanism that involves ion exchange and hydrophobic partitioning for monolayer composites as well as additional anion exchange in bilayer composites. Therefore, nonlinear isotherms for DCF adsorption on monolayer composites suggest an adsorption mechanism via both hydrophobic interactions between the alkyl chains of the O, D, C or A and the hydrophobic part of DCF, electrostatic interactions with the cationic heads from organic phase attached directly to the P surface as well as anion exchange of the counter anions in organic molecules from local bilayer with the anionic DCF. The improved DCF adsorption

capacities by bilayer composites demonstrated that anion exchange plays an important role throughout the entire adsorption process. The lowest adsorption of DCF by A composites (PAM and especially PAB) indicates that two alkyl chains in A are more densely packed and make the P surface more hydrophobic and prevent adsorption of an ionic form of DCF on the local bilayer in PAM and in complete bilayer in PAB. Although it was expected that composites with primary amine show lower adsorption of DCF, results indicated that these composites are good adsorbents for DCF. Overall results showed that the adsorption of DCF by composites containing different quaternary ammonium ions was dependent on the type of surfactant used for the modification of the P surface.

Figure 4 illustrates the influence of contact time on DCF adsorption onto O and D composites. According to the results, it can be seen that when the amount of organic phase utilized in the modification of P was 200% of ECEC values (PO200 and PD200), the adsorption rate increased rapidly (adsorption equilibrium was established in around 10–15 min). Adsorption of DCF was likewise fast for the PO100 sample, while for the PD100, adsorption of the drug was slower, and equilibrium was reached after approximately 45 min. For the initial concentration of DCF of 20 mg/L, maximum adsorbed amounts of the drug were 23.6 for PO200 and 19.1 mg/g for PD200, respectively, whereas maximum adsorbed values of DCF in composites with lower concentrations of organic phase were 13.0 mg/g and 8.5 mg/g, for PO100 and PD100, respectively.

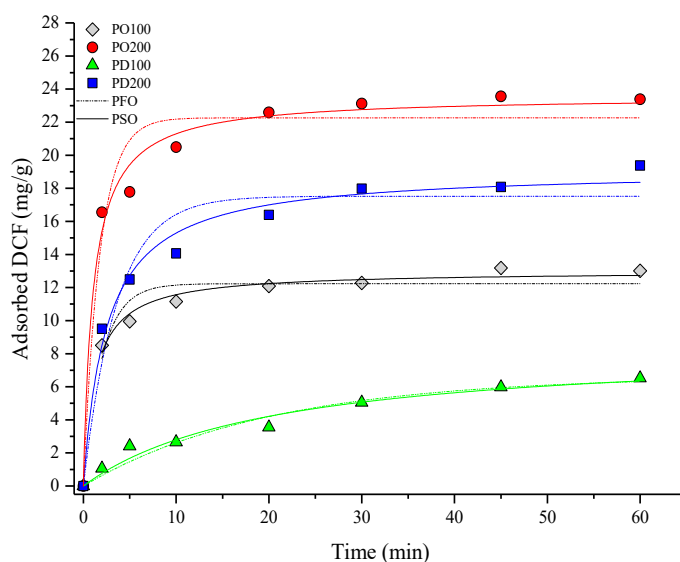


Figure 4. Kinetics run for DCF adsorption on composites of P. PFO = pseudo-first-order; PSO = pseudo-second-order.

The pseudo-first-order (PFO) and pseudo-second-order (PSO) models, which are denoted by Equations (3) and (4), are frequently used to analyze the kinetic runs for surfactant-modified minerals

$$Q_t = Q_{max} \left(1 - e^{-K_1 t}\right) \quad (3)$$

$$Q_t = \frac{K_2 Q_{max}^2 t}{K_2 Q_{max} t + 1} \quad (4)$$

where Q_{max} is the adsorbate concentration at equilibrium, Q_t is the amount of drug adsorbed by the adsorbent as a function of time t (min), and K_1 and K_2 are the pseudo-first and second-order constants, respectively.

According to statistical criteria (Table 4), PSO had a higher goodness-of-fit (correlation coefficients R^2). The PSO kinetics indicates that the chemical adsorption is the rate-determining step controlling DCF adsorption by O and D composites and is in agree-

ment with the results reported by other researchers [45,55,56] as well as with the kinetic results for the adsorption of DCF by C and A composites [29].

Table 4. Mathematical models of kinetic runs: parameters and goodness-of-fit.

Drug	Sample	Model	Parameters			Goodness-of-Fit	
			K_1 (min ⁻¹)	K_2 (g mg ⁻¹ min ⁻¹)	Q_{max} (mg/g)	R^2	AIC _w
DCF	PO100	PFO	0.5 ± 0.1		12.2 ± 0.4	0.676	0.005
		PSO		0.06 ± 0.01	13.0 ± 0.3	0.929	0.995
	PO200	PFO	0.6 ± 0.1		22.3 ± 0.8	0.950	0.006
		PSO		0.040 ± 0.008	23.6 ± 0.6	0.986	0.994
	PD100	PFO	0.05 ± 0.01		6.7 ± 0.7	0.952	0.225
		PSO		0.006 ± 0.002	8.5 ± 0.9	0.965	0.775
	PD200	PFO	0.27 ± 0.06		17.5 ± 0.8	0.937	0.005
		PSO		0.021 ± 0.004	19.1 ± 0.6	0.983	0.995

Composites prepared by modifying P with C had similar Q_{max} as composites with O (12.0 mg/g for PCM, 13.0 mg/g for PO100, 21.9 mg/g for PCB, and 23.6 mg/g for PO200). This additionally confirmed that the presence of the aromatic ring in the structure of both O and C as well similar chain length of these two surfactants, contribute to the higher adsorption of DCF. Among investigated surfactants, a composite with A had lower DCF capacities well as a composite with the primary amine—D. Thus, in the case of monolayer composites, DCF adsorbed amounts were 2.48 for PAM and 8.5 mg/g for PD100. However, adsorption kinetic was faster for PAM when equilibrium was reached after 10 min. For composites with an organic phase equal to 200% of ECEC, DCF adsorption was 13.1 and 19.1 mg/g for PAB and PD200, respectively.

2.3. Characterization after Adsorption: FTIR-ATR and Zeta Potential

In order to confirm the presence of DCF on O, D, C and A composites, the characterization of composite/drug complexes was performed by using FTIR spectroscopy and zeta potential measurements. Analyses were performed on samples collected after kinetic runs from this study (PO100, PO200, PD100, PD200) and also on samples from previous kinetic runs on DCF adsorption by PCM, PCB, PAM, and PAB [29].

Figure 5 shows the FTIR-ATR spectra for DCF and composites both before and after DCF adsorption. Similar behavior was noticed for all samples. According to the data, peaks at around 2920 cm⁻¹ and 2850 cm⁻¹ (symmetric and asymmetric C-H stretching vibrations) that originate from surfactant on the zeolitic surface were reduced after the adsorption of DCF. This most likely occurred due to the small desorption of the surfactant molecules that were weakly bonded at the zeolitic surface [47,57]. Additionally, low-intensity peaks in the spectra of O, D, C and A composites between 1590–1360 cm⁻¹ have appeared after drug adsorption, providing further evidence of DCF presence at the surfactants modified P surface. Namely, peaks assigned to asymmetric (1573 cm⁻¹) and symmetric stretching (1396 cm⁻¹) vibration of the carboxylate group in the DCF molecule (Figure 5A) were shifted after drug adsorption onto P composites. For composites with O and D, after adsorption of DCF, these vibrations were shifted to 1576 cm⁻¹ and 1376 cm⁻¹ (Figure 5B), and for composites containing C and A to 1576 cm⁻¹ and 1373 cm⁻¹ (Figure 5C). Similar behavior was reported for surfactant-modified bentonite [41] and kaolinite [58] after the adsorption of DCF, suggesting that the COO⁻ group is involved in drug adsorption onto composites. After drug incorporation, no appreciable changes in the wavenumbers of the bands ascribed to the P were seen, indicating that the zeolitic framework was unaffected by the drug adsorption. Similar behavior was reported in the case when salicylic acid was adsorbed on P composites (PCM, PCB, PAM, and PAB) [57], when IBU and DCF were adsorbed on composites of different minerals with O [13], and when IBU was adsorbed on composites of clinoptilolite-rich tuff with benzalkonium chloride and C [49].

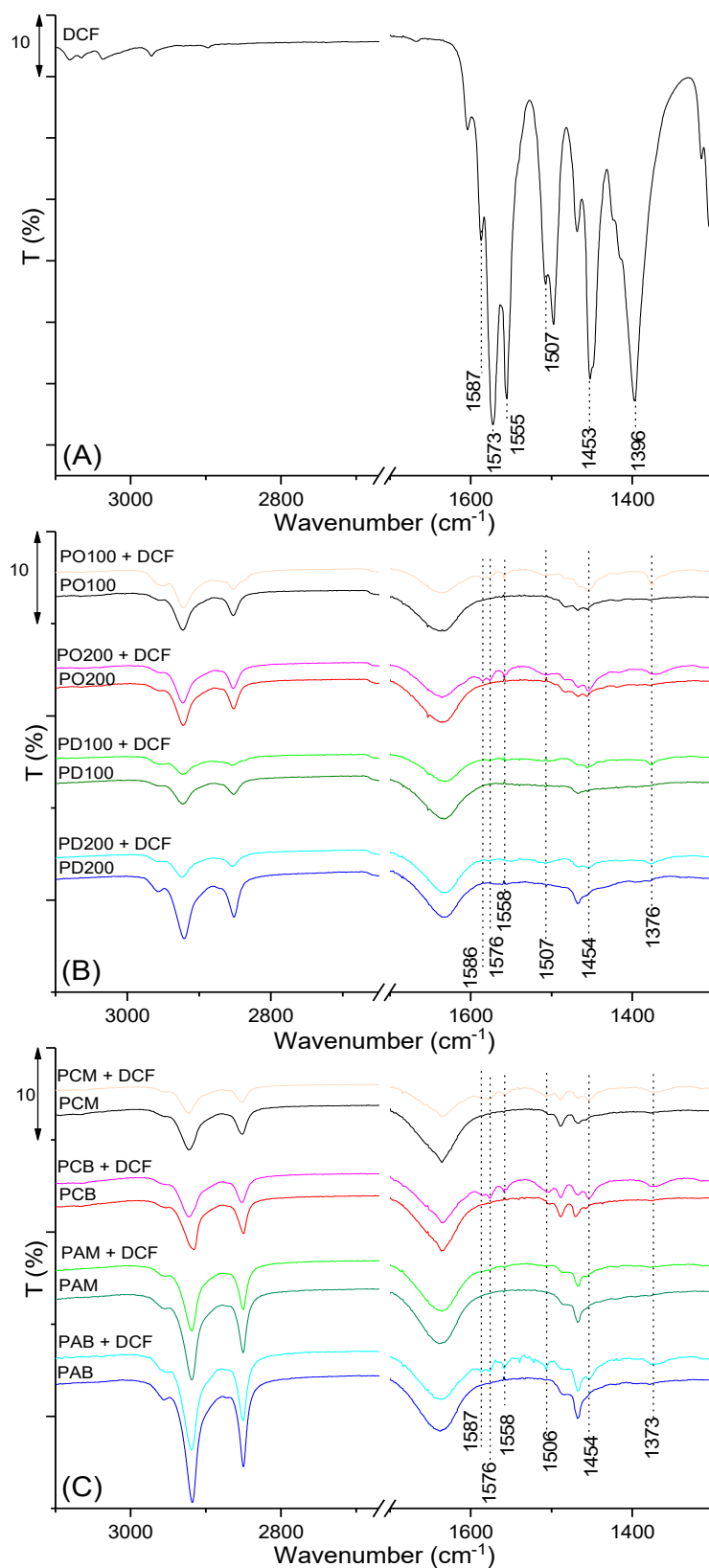


Figure 5. FTIR-ATR spectra of: DCF (A), spectra of P composites with dodecylamine and octadecyldimethylbenzylammonium chloride (PO100, PO200, PD100, and PD200) before and after adsorption of DCF (B), and spectra of P composites with cetylpyridinium chloride and Arquad[®]2HT-75 (PCM, PCB, PAM, and PAB) before and after adsorption of DCF [29] (C).

Results for the determination of the zeta potential of O, D, C and A composites before and after adsorption of DCF are presented in Figure 6. It can be seen that, after DCF adsorption, the zeta potential of the composite containing O altered from +2.3 mV to −3.4 mV for sample PO100 and from +20.2 mV to +15.5 mV in the case of PO200. When DCF was adsorbed on composites with D, zeta potential changed from −11.4 mV to −25.2 mV for sample PD100 and from −12.6 mV to −21.2 mV for sample PD200. Thus, when the amount of O, C, and A was equal to ECEC value (PO100, PCM, and PAM), the zeta potential was close to zero, confirming nearly monolayer formation and almost complete hydrophobicity of zeolitic surfaces. When the amount of both surfactants was 200% of the ECEC value, zeta potential became positive in the case of PO200, PCB, and PAB, pointing to charge reversal and bilayer formation at phillipsite surfaces. When D was used for modification potential of the phillipsite sample (PD100 and PD200) remained negative. After adsorption of DCF, zeta potential for all composites decreased: changed from positive to negative (PO100, PCM, PCB, and PAM), became more negative (PD100 and PD200), or became less positive (PO200 and PAB). The findings imply that the adsorption of DCF led to a change in the surface charge of composites, providing evidence that DCF molecules are present at the surface of O, D, C, and A composites. Differences in values of zeta potential after adsorption of DCF on P composites may be caused by the different arrangements of surfactant ions at their surfaces and are the consequence of the different structures of these molecules.

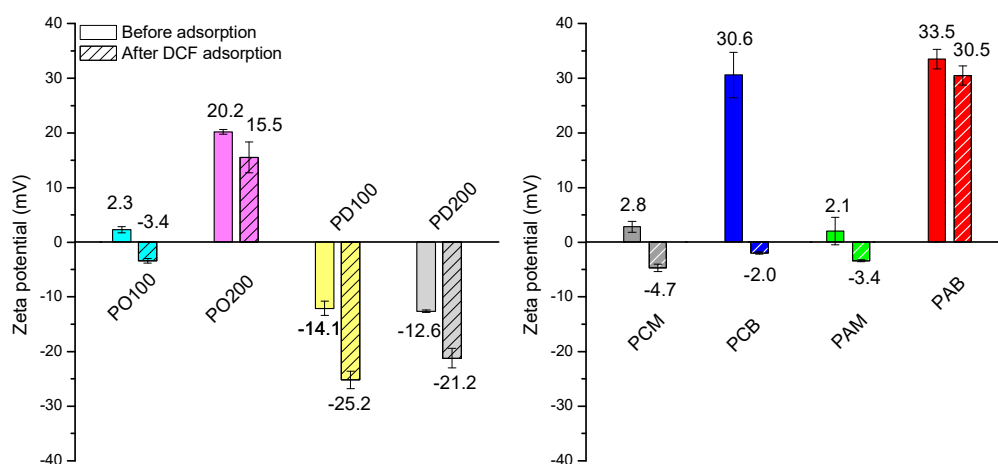


Figure 6. Zeta potential measured for P composites before and after adsorption of DCF. Measured values were compared with the zeta potential of the composites before drug adsorption previously reported in Smiljanic et al. (2020) [29]. Data were used with permission from Microporous and Mesoporous Materials, Elsevier, license number: 5436600349228.

3. Materials and Methods

In this study, natural zeolite (P) from Italy (trade name PHIL75) with 58% by weight of zeolite content was used as the starting material. The main zeolitic component of the tuff was phillipsite (44 wt%), whereas smaller amounts of analcime (10 wt%) and chabazite (4 wt%) were reported [29,47,59–61]. The ECEC value of the starting material was 0.13 mEq/g [62].

The surface of the zeolite-rich tuff was modified with the surfactants: quaternary ammonium salt—octadecyldimethylbenzylammonium chloride (O) (Hoechst AG, Frankfurt, Germany) and primary amine—dodecylamine (D) (Fluka, Buchs, Switzerland) (Figure 7). Two amounts of each surfactant equivalent to 100% or 200% of the external cation exchange capacity (ECEC) of the zeolite were used for the modification process. The composites were prepared according to the following procedure: 10 g of zeolite-rich tuff was added to 200 mL of distilled water containing surfactant equivalent to 100 and 200% ECEC zeolite.

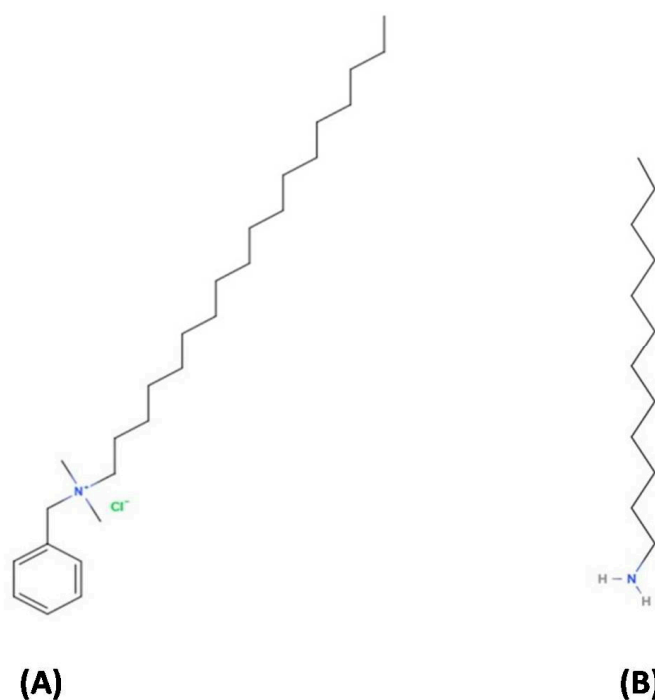


Figure 7. The structural formula of (A) octadecyldimethylbenzylammonium chloride (O) and (B) dodecylamine (D).

Modifications were made using a mixer at 6000 rotations per minute with a short activation time (about half an hour). When D was used to modify the zeolite surface to protonate the amino groups of the surfactant, the pH of the D solution was neutralized by the addition of 1M HCl. Composites of P with O are designated as PO, and the corresponding numbers 100 or 200 were added depending on the organic concentration, resulting in the composite names: PO100 and PO200. For composites of P and D, names were derived in the same manner: PD100 and PD200.

Several methods [13,29,62–64] were used to characterize the properties of the P and composites. FTIR spectra of starting material and both surfactants and composites before and after adsorption of the drug were collected using Nicolet iS50 spectrophotometer (Thermo Fisher Scientific, Waltham, MA, USA) with a diamond ATR accessory in the range 4000–400 cm^{-1} and with the resolution of 2 cm^{-1} and 32 scans. Starting material and prepared composites were characterized by simultaneous thermal analysis—STA (TGA/DSC). Prior to thermal analysis, all samples were dried for 2 h at 60 °C and then placed in a desiccator for 24 h at a relative humidity of 75%. The analysis was carried out in a synthetic air atmosphere (flow 70 mL/min), using PtRh crucibles, in the temperature range 25 °C–1000 °C with a heating rate of 10 °C/min (NETZSCH STA 449 F5 Jupiter, Selb, Germany). Additionally, the zeta potentials of starting material and composites before and after adsorption of the drug were measured using a Zetasizer Nano ZS90 (Malvern Instruments, Malvern, UK) that was calibrated using latex dispersion. Aqueous suspensions of 0.1 mg/mL for each material were prepared, and the mean value was calculated from 5 measurements.

The effect of contact time and initial drug concentration on DCF adsorption was studied in batch adsorption experiments following the procedures given by Smiljanic et al. (2020) [29]. The diclofenac sodium salt of the analytical grade ($\geq 98\%$) used in experiments was purchased from Sigma Aldrich (Schnellendorf, Germany). The stock solution of DCF (1000 mg/L) was prepared in methanol and then used to prepare 2–100 mg/L working solutions of the DCF in 0.01 M potassium phosphate buffer (pH 6.5). Suspensions were prepared by adding 10 mL of DCF working solutions (in various initial concentrations) to 5 mg of each composite. Suspensions were shaken for 60 min (time found sufficient to achieve

equilibrium conditions) at room temperature using a laboratory shaker (Heidolph Unimax 1010, Schwabach, Germany) with speed adjusted at 300 rpm. After adsorption, suspensions were filtered, and the concentration of DCF in filtrates was measured using UV–VIS spectroscopy (Spectrophotometer UV–1800, Shimadzu, Kyoto, Japan) at a wavelength of 276 nm. In order to carry out kinetic runs of DCF adsorption onto composites, 500 mg of each composite was added to 1000 mL of DCF water solution ($C_0 = 20$ mg/L, pH~6) and stirred for 60 min. At fixed time intervals, 5 mL aliquots were taken, filtered, and DCF concentration in filtrates was measured on UV–VIS.

The starting material-P used in this study was also used in the work of Smiljanic et al. (2020) [29] when cationic surfactants C and A served for modification of the mineral surface. Surfactant concentration was equivalent to 100% or 200% of zeolites' ECEC value, necessary for monolayer and bilayer formation, respectively, resulting in four composites with the following names [abbreviation used in the original work]: P+100% C [PCM], P+200% C [PCB], P+100% A [PAM], and P+200% A [PAB] [29]. Solid samples collected after kinetic runs in this study using composites (PO100, PO200, PD100, and PD200) and after kinetic runs performed in previous work (PCM, PCB, PAM, and PAB) were dried at room temperature and stored for further characterization. The zeta potential of all eight composites before and after DCF adsorption was evaluated using water suspension (0.1 g/L). Additionally, pure DCF and composites before and after DCF adsorption were characterized by FTIR spectroscopy.

4. Conclusions

Natural zeolite—phillipsite was modified with two different amounts of quaternary ammonium salt—O and primary amine—D, and composites were tested as adsorbents of the anti-inflammatory drug DCF. Results were compared with the adsorption of DCF by composites of phillipsite and quaternary ammonium salts—C and A. The effects of the type of surfactant, the initial concentration of the drug and the contact time on the adsorption of DCF were investigated. For O and D composites, adsorption of DCF increased with increasing the amount of each surfactant at the P surface as well as with increasing the initial concentration of the drug. The highest adsorption of DCF was achieved with PO200, which contains the highest amount of O. Comparison of results reported in this paper with previous results showed that adsorption of DCF by composites containing different quaternary ammonium ions (O, C and A) was dependent on the type of the surfactant used for the modification of the P surface. The presence of the aromatic ring in the structure of both O and C as well similar chain length of these two surfactants, contribute to the higher adsorption of DCF. Although it was expected that composites with primary amine—D would show lower adsorption of DCF, results indicated that these composites are good adsorbents for DCF and showed even higher adsorption of the drug than composites of P and surfactant-containing two alkyl chains (A). Overall results indicated that both composites of P with quaternary ammonium salt O or primary amine—D have the potential for removal of nonsteroidal anti-inflammatory drug DCF from contaminated water systems.

Author Contributions: Conceptualization, A.D.; formal analysis, M.O. (Milica Ožegović); investigation, D.S. and M.O. (Milena Obradović); resources, A.D.; data curation, M.M. and M.O. (Milena Obradović); writing—original draft preparation, D.S. and A.D.; writing—review and editing, A.D., M.M., G.E.R. and B.d.G.; visualization, M.O. (Milica Ožegović) and D.S.; supervision, A.D., B.d.G. and G.E.R. All authors have read and agreed to the published version of the manuscript.

Funding: This research was funded by the Ministry of Education, Science, and Technological Development of the Republic of Serbia, grant number 451-03-68/2022-14/200023.

Data Availability Statement: The data presented in this study are available on request from the corresponding author.

Conflicts of Interest: The authors declare no conflict of interest.

References

1. Inglezakis, V.J.; Zorpas, A.A. *Handbook of Natural Zeolites*; Bentham Science Publishers: Sharjah, United Arab Emirates, 2012. [[CrossRef](#)]
2. Smith, J.V. Definition of a Zeolite. *Zeolites* **1984**, *4*, 309–310. [[CrossRef](#)]
3. Delkash, M.; Ebrazi Bakhshayesh, B.; Kazemian, H. Using Zeolitic Adsorbents to Cleanup Special Wastewater Streams: A Review. *Microporous Mesoporous Mater.* **2015**, *214*, 224–241. [[CrossRef](#)]
4. Lemić, J.; Tomašević-Čanović, M.; Adamović, M.; Kovačević, D.; Miličević, S. Competitive Adsorption of Polycyclic Aromatic Hydrocarbons on Organo-Zeolites. *Microporous Mesoporous Mater.* **2007**, *105*, 317–323. [[CrossRef](#)]
5. Misaelides, P. Application of Natural Zeolites in Environmental Remediation: A Short Review. *Microporous Mesoporous Mater.* **2011**, *144*, 15–18. [[CrossRef](#)]
6. Erdem, E.; Karapinar, N.; Donat, R. The Removal of Heavy Metal Cations by Natural Zeolites. *J. Colloid Interface Sci.* **2004**, *280*, 309–314. [[CrossRef](#)] [[PubMed](#)]
7. Wang, S.; Peng, Y. Natural Zeolites as Effective Adsorbents in Water and Wastewater Treatment. *Chem. Eng. J.* **2010**, *156*, 11–24. [[CrossRef](#)]
8. Albino, V.; Cioffi, R.; Pansini, M.; Colella, C. Disposal of Lead-Containing Zeolite Sludges in Cement Matrix. *Environ. Technol.* **1995**, *16*, 147–156. [[CrossRef](#)]
9. Cioffi, R.; Pansini, M.; Caputo, D.; Colella, C. Evaluation of Mechanical and Leaching Properties of Cement-Based Solidified Materials Encapsulating Cd-Exchanged Natural Zeolites. *Environ. Technol.* **1996**, *17*, 1215–1224. [[CrossRef](#)]
10. Colella, C.; de' Gennaro, M.; Langella, A.; Pansini, M. Evaluation of Natural Phillipsite and Chabazite as Cation Exchangers for Copper and Zinc. *Sep. Sci. Technol.* **1998**, *33*, 467–481. [[CrossRef](#)]
11. Pansini, M.; Colella, C. Dynamic Data on Lead Uptake from Water by Chabazite. *Desalination* **1990**, *78*, 287–295. [[CrossRef](#)]
12. Haggerty, G.M.; Bowman, R.S. Sorption of Chromate and Other Inorganic Anions by Organo-Zeolite. *Environ. Sci. Technol.* **1994**, *28*, 452–458. [[CrossRef](#)] [[PubMed](#)]
13. Obradović, M.; Daković, A.; Smiljanić, D.; Ožegović, M.; Marković, M.; Rottinghaus, G.E.; Krstić, J. Ibuprofen and Diclofenac Sodium Adsorption onto Functionalized Minerals: Equilibrium, Kinetic and Thermodynamic Studies. *Microporous Mesoporous Mater.* **2022**, *335*, 111795. [[CrossRef](#)]
14. De Gennaro, B.; Mercurio, M.; Cappelletti, P.; Catalanotti, L.; Daković, A.; De Bonis, A.; Grifa, C.; Izzo, F.; Kraković, M.; Monetti, V.; et al. Use of Surface Modified Natural Zeolite (SMNZ) in Pharmaceutical Preparations. Part 2. A New Approach for a Fast Functionalization of Zeolite-Rich Carriers. *Microporous Mesoporous Mater.* **2016**, *235*, 42–49. [[CrossRef](#)]
15. Cappelletti, P.; Colella, A.; Langella, A.; Mercurio, M.; Catalanotti, L.; Monetti, V.; de Gennaro, B. Use of Surface Modified Natural Zeolite (SMNZ) in Pharmaceutical Preparations Part 1. Mineralogical and Technological Characterization of Some Industrial Zeolite-Rich Rocks. *Microporous Mesoporous Mater.* **2017**, *250*, 232–244. [[CrossRef](#)]
16. Reeve, P.J.; Fallowfield, H.J. The Toxicity of Cationic Surfactant HDTMA-Br, Desorbed from Surfactant Modified Zeolite, towards Faecal Indicator and Environmental Microorganisms. *J. Hazard. Mater.* **2017**, *339*, 208–215. [[CrossRef](#)] [[PubMed](#)]
17. Li, Z.; Bowman, R.S. Sorption of Perchloroethylene by Surfactant-Modified Zeolite as Controlled by Surfactant Loading. *Environ. Sci. Technol.* **1998**, *32*, 2278–2282. [[CrossRef](#)]
18. Mirzaei, N.; Hadi, M.; Gholami, M.; Fard, R.F.; Aminabad, M.S. Sorption of Acid Dye by Surfactant Modified Natural Zeolites. *J. Taiwan Inst. Chem. Eng.* **2016**, *59*, 186–194. [[CrossRef](#)]
19. Schulze-Makuch, D.; Pillai, S.D.; Guan, H.; Bowman, R.; Couroux, E.; Hielscher, F.; Totten, J.; Espinosa, I.Y.; Kretzschmar, T. Surfactant-Modified Zeolite Can Protect Drinking Water Wells from Viruses and Bacteria. *EOS* **2002**, *83*, 193–201. [[CrossRef](#)]
20. Zhan, Y.; Lin, J.; Qiu, Y.; Gao, N.; Zhu, Z. Adsorption of Humic Acid from Aqueous Solution on Bilayer Hexadecyltrimethyl Ammonium Bromide-Modified Zeolite. *Front. Environ. Sci. Eng. China* **2011**, *5*, 65–75. [[CrossRef](#)]
21. Bowman, R.S. Applications of Surfactant-Modified Zeolites to Environmental Remediation. *Microporous Mesoporous Mater.* **2003**, *61*, 43–56. [[CrossRef](#)]
22. De Gennaro, B. Surface modification of zeolites for environmental applications. In *Modified Clay and Zeolite Nanocomposite Materials: Environmental and Pharmaceutical Applications*; Elsevier Inc.: Amsterdam, The Netherlands, 2018; pp. 57–85. [[CrossRef](#)]
23. De Gennaro, B.; Catalanotti, L.; Bowman, R.S.; Mercurio, M. Anion Exchange Selectivity of Surfactant Modified Clinoptilolite-Rich Tuff for Environmental Remediation. *J. Colloid Interface Sci.* **2014**, *430*, 178–183. [[CrossRef](#)] [[PubMed](#)]
24. De Gennaro, B.; Aprea, P.; Liguori, B.; Galzerano, B.; Peluso, A.; Caputo, D. Zeolite-Rich Composite Materials for Environmental Remediation: Arsenic Removal from Water. *Appl. Sci.* **2020**, *10*, 6939. [[CrossRef](#)]
25. Dimas Rivera, G.L.; Martínez Hernández, A.; Pérez Cabello, A.F.; Rivas Barragán, E.L.; Liñán Montes, A.; Flores Escamilla, G.A.; Sandoval Rangel, L.; Suarez Vazquez, S.I.; De Haro Del Río, D.A. Removal of Chromate Anions and Immobilization Using Surfactant-Modified Zeolites. *J. Water Process Eng.* **2020**, *39*, 101717. [[CrossRef](#)]
26. Apreutesei, R.E.; Catrinescu, C.; Teodosiu, C. Surfactant-Modified Natural Zeolites for Environmental Applications in Water Purification. *Environ. Eng. Manag. J.* **2008**, *7*, 149–161. [[CrossRef](#)]
27. Hrenovic, J.; Rozic, M.; Sekovanic, L.; Anic-Vucinic, A. Interaction of Surfactant-Modified Zeolites and Phosphate Accumulating Bacteria. *J. Hazard. Mater.* **2008**, *156*, 576–582. [[CrossRef](#)]

28. Smiljanić, D.; de Gennaro, B.; Daković, A.; Galzerano, B.; Germinario, C.; Izzo, F.; Rottinghaus, G.E.; Langella, A. Removal of Non-Steroidal Anti-Inflammatory Drugs from Water by Zeolite-Rich Composites: The Interference of Inorganic Anions on the Ibuprofen and Naproxen Adsorption. *J. Environ. Manage.* **2021**, *286*, 112168. [[CrossRef](#)]
29. Smiljanić, D.; de Gennaro, B.; Izzo, F.; Langella, A.; Daković, A.; Germinario, C.; Rottinghaus, G.E.; Spasojević, M. Removal of Emerging Contaminants from Water by Zeolite-Rich Composites: A First Approach Aiming at Diclofenac and Ketoprofen. *Microporous Mesoporous Mater.* **2020**, *289*, 110057. [[CrossRef](#)]
30. Burian, M.; Geisslinger, G. COX-Dependent Mechanisms Involved in the Antinociceptive Action of NSAIDs at Central and Peripheral Sites. *Pharmacol. Ther.* **2005**, *107*, 139–154. [[CrossRef](#)]
31. Jung, C.; Boateng, L.K.; Flora, J.R.V.; Oh, J.; Braswell, M.C.; Son, A.; Yoon, Y. Competitive Adsorption of Selected Non-Steroidal Anti-Inflammatory Drugs on Activated Biochars: Experimental and Molecular Modeling Study. *Chem. Eng. J.* **2015**, *264*, 1–9. [[CrossRef](#)]
32. Gros, M.; Petrović, M.; Ginebreda, A.; Barceló, D. Removal of Pharmaceuticals during Wastewater Treatment and Environmental Risk Assessment Using Hazard Indexes. *Environ. Int.* **2010**, *36*, 15–26. [[CrossRef](#)]
33. Lonappan, L.; Brar, S.K.; Das, R.K.; Verma, M.; Surampalli, R.Y. Diclofenac and Its Transformation Products: Environmental Occurrence and Toxicity—A Review. *Environ. Int.* **2016**, *96*, 127–138. [[CrossRef](#)] [[PubMed](#)]
34. Loos, R.; Carvalho, R.; António, D.C.; Comero, S.; Locoro, G.; Tavazzi, S.; Paracchini, B.; Ghiani, M.; Lettieri, T.; Blaha, L.; et al. EU-Wide Monitoring Survey on Emerging Polar Organic Contaminants in Wastewater Treatment Plant Effluents. *Water Res.* **2013**, *47*, 6475–6487. [[CrossRef](#)]
35. Sousa, J.C.G.; Ribeiro, A.R.; Barbosa, M.O.; Pereira, M.F.R.; Silva, A.M.T. A Review on Environmental Monitoring of Water Organic Pollutants Identified by EU Guidelines. *J. Hazard. Mater.* **2018**, *344*, 146–162. [[CrossRef](#)] [[PubMed](#)]
36. Yang, Y.; Ok, Y.S.; Kim, K.H.; Kwon, E.E.; Tsang, Y.F. Occurrences and Removal of Pharmaceuticals and Personal Care Products (PPCPs) in Drinking Water and Water/Sewage Treatment Plants: A Review. *Sci. Total Environ.* **2017**, *596–597*, 303–320. [[CrossRef](#)]
37. Oaks, J.L.; Meteyer, C.U.; Rideout, B.A.; Shivaprasad, H.L.; Gilbert, M.; Virani, M.; Watson, R.T.; Khan, A.A. Diagnostic Investigation of Vulture Mortality: The Anti-Inflammatory Drug Diclofenac Is Associated with Visceral Gout. In Proceedings of the Raptor Worldwide, 6th World Conference on Birds of Prey and Owls, Budapest, Hungary, 18–23 May 2003; pp. 241–243.
38. Balmford, A. Pollution, Politics, and Vultures. *Science* **2013**, *339*, 653–655. [[CrossRef](#)]
39. Bonnefille, B.; Gomez, E.; Courant, F.; Escande, A.; Fenet, H. Diclofenac in the Marine Environment: A Review of Its Occurrence and Effects. *Mar. Pollut. Bull.* **2018**, *131*, 496–506. [[CrossRef](#)]
40. De Oliveira, T.; Guégan, R.; Thiebault, T.; Le Milbeau, C.; Muller, F.; Teixeira, V.; Giovanela, M.; Boussafir, M. Adsorption of Diclofenac onto Organoclays: Effects of Surfactant and Environmental (PH and Temperature) Conditions. *J. Hazard. Mater.* **2017**, *323*, 558–566. [[CrossRef](#)]
41. França, D.B.; Trigueiro, P.; Silva Filho, E.C.; Fonseca, M.G.; Jaber, M. Monitoring Diclofenac Adsorption by Organophilic Alkylpyridinium Bentonites. *Chemosphere* **2020**, *242*, 125109. [[CrossRef](#)]
42. Maia, G.S.; de Andrade, J.R.; da Silva, M.G.C.; Vieira, M.G.A. Adsorption of Diclofenac Sodium onto Commercial Organoclay: Kinetic, Equilibrium and Thermodynamic Study. *Powder Technol.* **2019**, *345*, 140–150. [[CrossRef](#)]
43. Sun, K.; Shi, Y.; Wang, X.; Li, Z. Sorption and Retention of Diclofenac on Zeolite in the Presence of Cationic Surfactant. *J. Hazard. Mater.* **2017**, *323*, 584–592. [[CrossRef](#)]
44. Izzo, F.; Mercurio, M.; de Gennaro, B.; Aprea, P.; Cappelletti, P.; Daković, A.; Germinario, C.; Grifa, C.; Smiljanic, D.; Langella, A. Surface Modified Natural Zeolites (SMNZs) as Nanocomposite Versatile Materials for Health and Environment. *Colloids Surfaces B Biointerfaces* **2019**, *182*, 110380. [[CrossRef](#)]
45. Mercurio, M.; Izzo, F.; Langella, A.; Grifa, C.; Germinario, C.; Daković, A.; Aprea, P.; Pasquino, R.; Cappelletti, P.; Graziano, F.S.; et al. Surface-Modified Phillipsite-Rich Tuff from the Campania Region (Southern Italy) as a Promising Drug Carrier: An Ibuprofen Sodium Salt Trial. *Am. Mineral.* **2018**, *103*, 700–710. [[CrossRef](#)]
46. Govindasamy, P.; Gunasekaran, S. Quantum Mechanical Calculations and Spectroscopic (FT-IR, FT-Raman and UV) Investigations, Molecular Orbital, NLO, NBO, NLMO and MESP Analysis of 4-[5-(4-Methylphenyl)-3-(Trifluoromethyl)-1H-Pyrazol-1-Yl] Benzene-1-Sulfonamide. *J. Mol. Struct.* **2015**, *1081*, 96–109. [[CrossRef](#)]
47. Marković, M.; Daković, A.; Krajišnik, D.; Kragović, M.; Milić, J.; Langella, A.; de Gennaro, B.; Cappelletti, P.; Mercurio, M. Evaluation of the Surfactant/Phillipsite Composites as Carriers for Diclofenac Sodium. *J. Mol. Liq.* **2016**, *222*, 711–716. [[CrossRef](#)]
48. Krajišnik, D.; Daković, A.; Milojević, M.; Malenović, A.; Kragović, M.; Bogdanović, D.B.; Dondur, V.; Milić, J. Properties of Diclofenac Sodium Sorption onto Natural Zeolite Modified with Cetylpyridinium Chloride. *Colloids Surfaces B Biointerfaces* **2011**, *83*, 165–172. [[CrossRef](#)]
49. Krajišnik, D.; Daković, A.; Malenović, A.; Kragović, M.; Milić, J. Ibuprofen Sorption and Release by Modified Natural Zeolites as Prospective Drug Carriers. *Clay Miner.* **2015**, *50*, 11–22. [[CrossRef](#)]
50. Del Orta, M.M.; Flores, F.M.; Morantes, C.F.; Curutchet, G.; Torres Sánchez, R.M. Interrelations of Structure, Electric Surface Charge, and Hydrophobicity of Organo-Mica and -Montmorillonite, Tailored with Quaternary or Primary Amine Cations. Preliminary Study of Pyrimethanil Adsorption. *Mater. Chem. Phys.* **2019**, *223*, 325–335. [[CrossRef](#)]
51. Foo, K.Y.; Hameed, B.H. Insights into the Modeling of Adsorption Isotherm Systems. *Chem. Eng. J.* **2010**, *156*, 2–10. [[CrossRef](#)]

52. Santhana Krishna Kumar, A.; Ramachandran, R.; Kalidhasan, S.; Rajesh, V.; Rajesh, N. Potential Application of Dodecylamine Modified Sodium Montmorillonite as an Effective Adsorbent for Hexavalent Chromium. *Chem. Eng. J.* **2012**, *211–212*, 396–405. [[CrossRef](#)]
53. Spiess, A.-N.; Neumeyer, N. An Evaluation of R2 as an Inadequate Measure for Nonlinear Models in Pharmacological and Biochemical Research: A Monte Carlo Approach. *BMC Pharmacol.* **2010**, *10*, 6. [[CrossRef](#)]
54. Glatting, G.; Kletting, P.; Reske, S.N.; Hohl, K.; Ring, C. Choosing the Optimal Fit Function: Comparison of the Akaike Information Criterion and the F-Test. *Med. Phys.* **2007**, *34*, 4285–4292. [[CrossRef](#)]
55. Malvar, J.L.; Martín, J.; del Orta, M.M.; Medina-Carrasco, S.; Santos, J.L.; Aparicio, I.; Alonso, E. Simultaneous and Individual Adsorption of Ibuprofen Metabolites by a Modified Montmorillonite. *Appl. Clay Sci.* **2020**, *189*, 105529. [[CrossRef](#)]
56. Ghemit, R.; Makhloufi, A.; Djebri, N.; Fililissa, A.; Zerroual, L.; Boutahala, M. Adsorptive Removal of Diclofenac and Ibuprofen from Aqueous Solution by Organobentonites: Study in Single and Binary Systems. *Groundw. Sustain. Dev.* **2019**, *8*, 520–529. [[CrossRef](#)]
57. Smiljanić, D.; Daković, A.; Obradović, M.; Ožegović, M.; Izzo, F.; Germinario, C.; de Gennaro, B. Application of Surfactant Modified Natural Zeolites for the Removal of Salicylic Acid—A Contaminant of Emerging Concern. *Materials* **2021**, *14*, 7728. [[CrossRef](#)]
58. Sun, K.; Shi, Y.; Wang, X.; Rasmussen, J.; Li, Z.; Zhu, J. Organokaolin for the Uptake of Pharmaceuticals Diclofenac and Chloramphenicol from Water. *Chem. Eng. J.* **2017**, *330*, 1128–1136. [[CrossRef](#)]
59. De Gennaro, B.; Aprea, P.; Pepe, F.; Colella, C. Cation Selectivity of a Ca²⁺ Pre-Exchanged Clinoptilolite Tuff. *Stud. Surf. Sci. Catal.* **2007**, *170*, 2128–2133. [[CrossRef](#)]
60. de Gennaro, B.; Aprea, P.; Colella, C.; Buondonno, A. Comparative Ion-Exchange Characterization of Zeolitic and Clayey Materials for Pedotechnical Applications-Part 2: Interaction with Nutrient Cations. *J. Porous Mater.* **2007**, *16*, 667–673. [[CrossRef](#)]
61. De Gennaro, B.; Colella, A.; Cappelletti, P.; Pansini, M.; de' Gennaro, M.; Colella, C. Effectiveness of Clinoptilolite in Removing Toxic Cations from Water: A Comparative Study. *Stud. Surf. Sci. Catal.* **2005**, *158B*, 1153–1160. [[CrossRef](#)]
62. Marković, M.; Daković, A.; Rottinghaus, G.E.; Kragović, M.; Petković, A.; Krajišnik, D.; Milić, J.; Mercurio, M.; de Gennaro, B. Adsorption of the Mycotoxin Zearalenone by Clinoptilolite and Phillipsite Zeolites Treated with Cetylpyridinium Surfactant. *Colloids Surf. B Biointerfaces* **2017**, *151*, 324–332. [[CrossRef](#)]
63. Zhu, S.; Khan, M.A.; Kameda, T.; Xu, H.; Wang, F.; Xia, M.; Yoshioka, T. New Insights into the Capture Performance and Mechanism of Hazardous Metals Cr³⁺ and Cd²⁺ onto an Effective Layered Double Hydroxide Based Material. *J. Hazard. Mater.* **2022**, *426*, 128062. [[CrossRef](#)]
64. Zhu, S.; Xia, M.; Chu, Y.; Khan, M.A.; Lei, W.; Wang, F.; Muhmood, T.; Wang, A. Adsorption and Desorption of Pb(II) on L-Lysine Modified Montmorillonite and the Simulation of Interlayer Structure. *Appl. Clay Sci.* **2019**, *169*, 40–47. [[CrossRef](#)]

Disclaimer/Publisher's Note: The statements, opinions and data contained in all publications are solely those of the individual author(s) and contributor(s) and not of MDPI and/or the editor(s). MDPI and/or the editor(s) disclaim responsibility for any injury to people or property resulting from any ideas, methods, instructions or products referred to in the content.